

Supporting Information

Nanoporous In-MOF with Multiple One-Dimensional Pores

**Seong Huh^{a,*} Tae-Hwan Kwon,^a Noejung Park,^{b,*} Sung-Jin Kim^c
and Youngmee Kim^{c,*}**

^a *Department of Chemistry and Protein Research Center for Bio-Industry, Hankuk University of Foreign Studies, Yongin 449-791, Korea, Fax: 82 31 330 4566; Tel: 82 31 330 4522; E-mail: shuh@hufs.ac.kr.*

^b *Department of Applied Physics, Dankook University, Yongin-si, Gyeonggi-do, 448-701, Korea, E-mail: noejung@dku.edu.*

^c *Department of Chemistry and Nano Science, Ewha Womans University, Seoul 120-750, Korea. E-mail: ymeekim@ewha.ac.kr.*

Preparation of (Et₂NH₂)[In(2,6-NDC)₂·2H₂O·DEF] (1)

InCl₃ (0.221 g, 1.0 mmol, Aldrich), 2,6-naphthalenedicarboxylic acid (0.432 g, 2.0 mmol, TCI), and 20 mL of *N,N*-diethylformamide (TCI) were sealed in a Teflon-lined high pressure bomb and heated at 130°C for 144 h. After slow cooling to room temperature, the colorless crystalline solids were retrieved by filtration and washed with diethylformamide. The as-made solids were immediately immersed in 20 mL of chloroform for the CHCl₃-exchanged sample. High quality colorless needles were chosen for the X-ray crystallography from the as-made sample.

X-ray Crystallography

The diffraction data for **1** were collected on a Bruker SMART AXS diffractometer using Mo K α ($\lambda = 0.71073$ Å). The crystal was mounted on a glass fiber under epoxy. The CCD data were integrated and scaled using a Bruker SAINT, and the structures were

solved and refined using SHELXTL. Hydrogen atoms were located in the calculated positions. The crystallographic data are listed in Table S1. The selected bond lengths and angles are listed in Table S2. The CIF deposition number: CCDC 646877.

Physical Measurements

The N₂ sorption analysis was performed on a Belsorp-miniII at 77 K (BEL Japan). The samples were dried at 393 K under high vacuum for 2 h. Low-pressure hydrogen adsorption measurements were performed at 77 K on a Belsorp-miniII. The equipment was calibrated by using Cu-BTC (HKUST-1) as a reference material (S. S. -Y. Chui et al., *Science* 1999, **283**, 1148). The as-made HKUST-1 activated at 393 K under high vacuum for 2 h showed hydrogen uptake value of 2.23 wt% at 77 K and 1 bar. This value agrees well with the reported value (2.27 wt%) under the same condition (B. Xiao et al., *J. Am. Chem. Soc.*, 2007, **129**, 1203). Powder X-ray diffraction patterns were obtained by using a Rigaku MiniFlex (30 kV, 15 mA). Thermogravimetric analysis was carried out on a TGA Q5000 (TA Instruments) under nitrogen atmosphere.

Table S1. Crystal data and structure refinement for **1**.

Empirical formula	$C_{33} H_{38} In N_2 O_{11}$	
Formula weight	753.48	
Temperature	170(2) K	
Wavelength	0.71073 Å	
Crystal system	Tetragonal	
Space group	P4/n	
Unit cell dimensions	$a = 31.745(3) \text{ \AA}$	$\alpha = 90.00^\circ$
	$b = 31.745(3) \text{ \AA}$	$\beta = 90.00^\circ$
	$c = 8.2835(15) \text{ \AA}$	$\gamma = 90.00^\circ$
Volume	$8347.9(19) \text{ \AA}^3$	
Z	8	
Density (calculated)	1.193 Mg/m^3	
Absorption coefficient	0.616 mm^{-1}	
F(000)	3064	
Crystal size	$0.25 \times 0.08 \times 0.08 \text{ mm}^3$	
Theta range for data collection	1.81 to 25.99	
Index ranges	$-39 \leq h \leq 28, -39 \leq k \leq 38, -10 \leq l \leq 9$	
Reflections collected	44090	
Independent reflections	8208 [R(int) = 0.1435]	
Completeness to theta = 25.99	100.0 %	
Refinement method	Full-matrix least-squares on F ²	
Data / restraints / parameters	8208 / 0 / 418	
Goodness-of-fit on F ²	1.089	
Final R indices [I > 2σ(I)]	$R_1 = 0.0998, wR_2 = 0.2668$	
R indices (all data)	$R_1 = 0.1460, wR_2 = 0.2812$	
Largest diff. peak and hole	$1.521 \text{ and } -2.405 \text{ e.\AA}^{-3}$	

Table S2. Selected bond lengths [Å] and angles [°] for **1**.

In(1)-O(14)	2.186(7)
In(1)-O(22)	2.234(7)
In(1)-O(23)	2.241(7)
In(1)-O(11)	2.242(7)
In(1)-O(12)	2.259(7)
In(1)-O(24)	2.286(7)
In(1)-O(21)	2.300(7)
In(1)-O(13)	2.397(7)
O(14)-In(1)-O(22)	89.9(3)
O(14)-In(1)-O(23)	141.5(3)
O(22)-In(1)-O(23)	85.2(3)
O(14)-In(1)-O(11)	86.0(3)
O(22)-In(1)-O(11)	164.3(3)
O(23)-In(1)-O(11)	88.6(2)
O(14)-In(1)-O(12)	86.5(3)
O(22)-In(1)-O(12)	137.1(3)
O(23)-In(1)-O(12)	121.9(3)
O(11)-In(1)-O(12)	57.8(3)
O(14)-In(1)-O(24)	160.7(3)
O(22)-In(1)-O(24)	88.1(3)
O(23)-In(1)-O(24)	57.4(3)
O(11)-In(1)-O(24)	100.6(3)
O(12)-In(1)-O(24)	82.0(3)
O(14)-In(1)-O(21)	80.7(3)
O(22)-In(1)-O(21)	57.2(3)
O(23)-In(1)-O(21)	126.1(3)
O(11)-In(1)-O(21)	136.5(3)
O(12)-In(1)-O(21)	80.1(3)
O(24)-In(1)-O(21)	82.1(3)
O(14)-In(1)-O(13)	56.6(3)
O(22)-In(1)-O(13)	79.7(3)
O(23)-In(1)-O(13)	85.0(3)
O(11)-In(1)-O(13)	85.4(3)
O(12)-In(1)-O(13)	130.4(3)
O(24)-In(1)-O(13)	141.4(2)
O(21)-In(1)-O(13)	119.2(2)

Table S3. The result of interpenetrating modes analyzed by TOPOS (Topos 4.0 Pro).

#####

1:C33 H38 In N2 O11

#####

Topology for In1

Atom In1 links by bridge ligands and has

Common vertex with					R(A-A)	f
In 1	0.8070	0.5346	-0.9031	(1 0-1)	12.988A	1
In 1	0.6930	0.9654	1.0969	(0 1 1)	12.988A	1
In 1	0.1930	0.4654	-0.0969	(-1 1 0)	13.128A	1
In 1	0.3070	1.0346	-0.0969	(1 0 0)	13.128A	1

Structural group analysis

Structural group No 1

Structure consists of 3D framework with InO₈C₂₄H₁₂

There are 4 interpenetrating nets

FIV: Full interpenetration vectors

[0,0,1] (8.28A)

PIC: [0,0,4][0,1,-2][1,1,0] (PICVR=4)

Zt=4; Zn=1

Class Ia Z=4

Coordination sequences

In1:	1	2	3	4	5	6	7	8	9	10
Num	4	9	18	32	48	67	92	120	150	185
Cum	5	14	32	64	112	179	271	391	541	726

TD10=726

Vertex symbols for selected sublattice

In1 Point (Schläfli) symbol: {4³.6².8}

Extended point symbol: [4.4.4.8(3).6.6]

Vertex symbol: [4.4.4.8(2).8.8]

All rings (up to 10): coincide with rings

All rings with types: [4b.4b.4a.8(2).8.8]

Point (Schläfli) symbol for net: {4³.6².8}

4-c net; uninodal net

Topological type: gis Gismondine GIS; 4/4/t3; sqc2200 (topos&RCSR.ttd) {4³.6².8} - VS
[4.4.4.8(2).8.8] (66909 types in 9 databases)

Essential rings by homocrossing: 4a,4b,8

Inessential rings by homocrossing: none

Rings crossed by bonds: 8

Proper tiling cannot be constructed. Not all edges are shared.

Table S4. Binding energy of the hydrogen molecule onto various sites of **1** and MOF-5.

	Computational Method	Binding Energy (eV)
In-MOF with H ₂ on site A	GGA	0.05
In-MOF with H ₂ on site B	GGA	0.07
In-MOF with H ₂ on site C	GGA	0.09
In-MOF with H ₂ on site C	LDA	0.13
MOF-5 with H ₂ near oxygen	GGA	0.02
MOF-5 with H ₂ near oxygen	LDA	0.11

Figure S1. Coordination environment of the In(III) ion showing a T-motif.

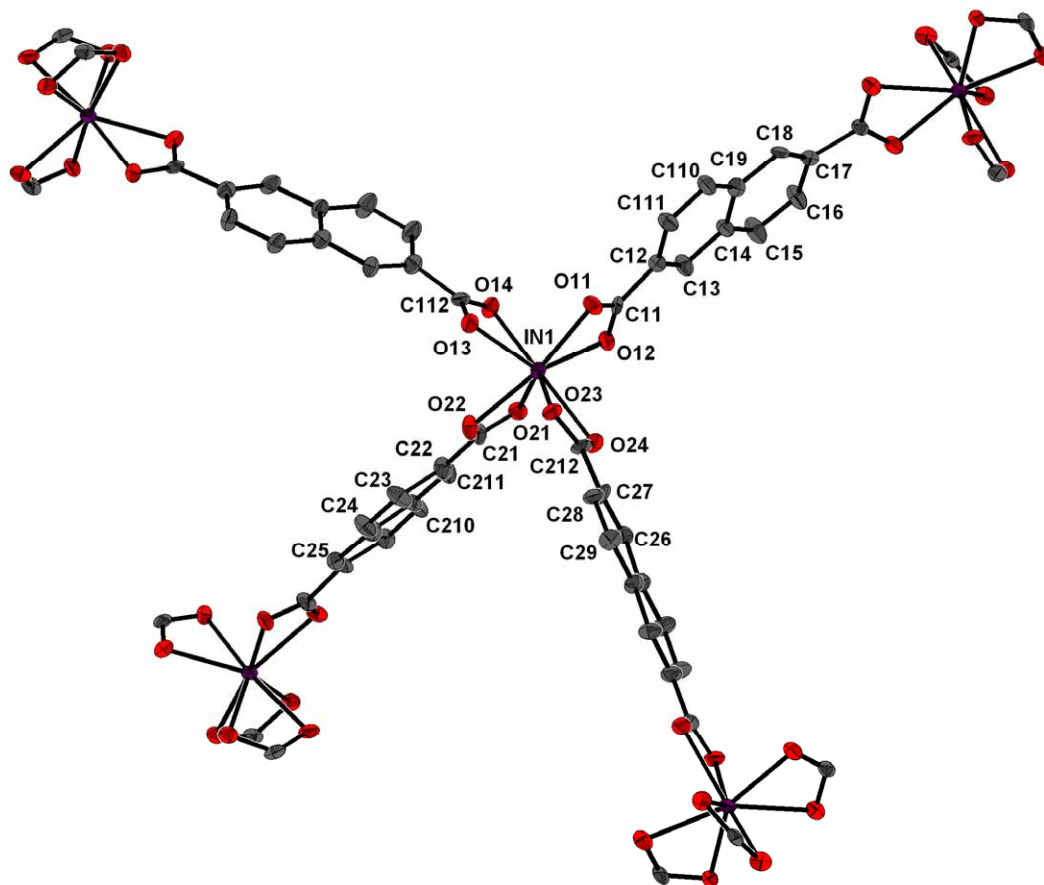


Figure S2. Connolly surface of **1** with a probe radius of 1.4 Å (a) and pore dimensions for the three 1D channels in Å (b).

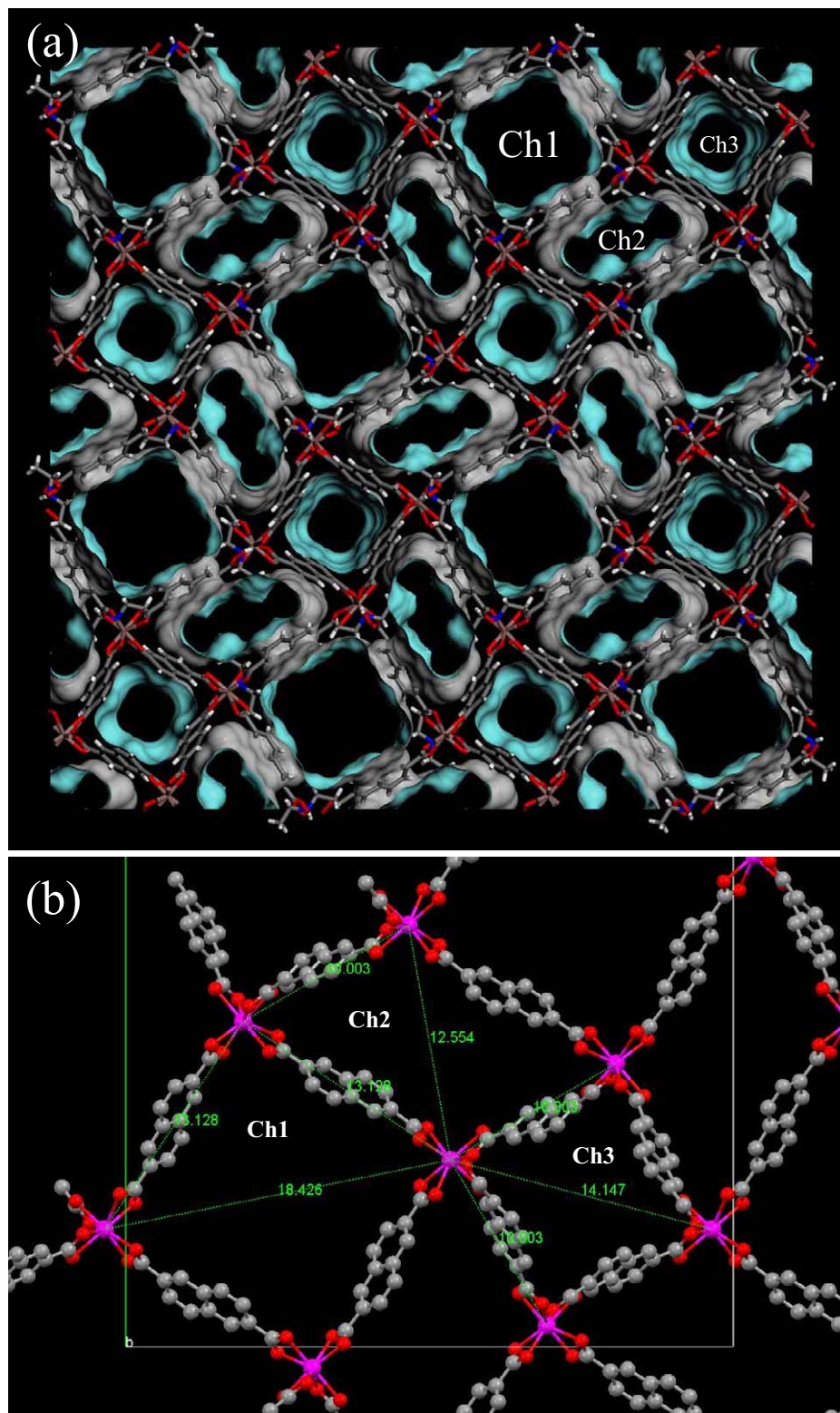


Figure S3. The detailed structure of the Ch1 with two water solvates (oxygen atoms as red spheres), a DEF, and an Et_2NH_2^+ ion: a view along c -axis (a) and a view along a -axis (b).

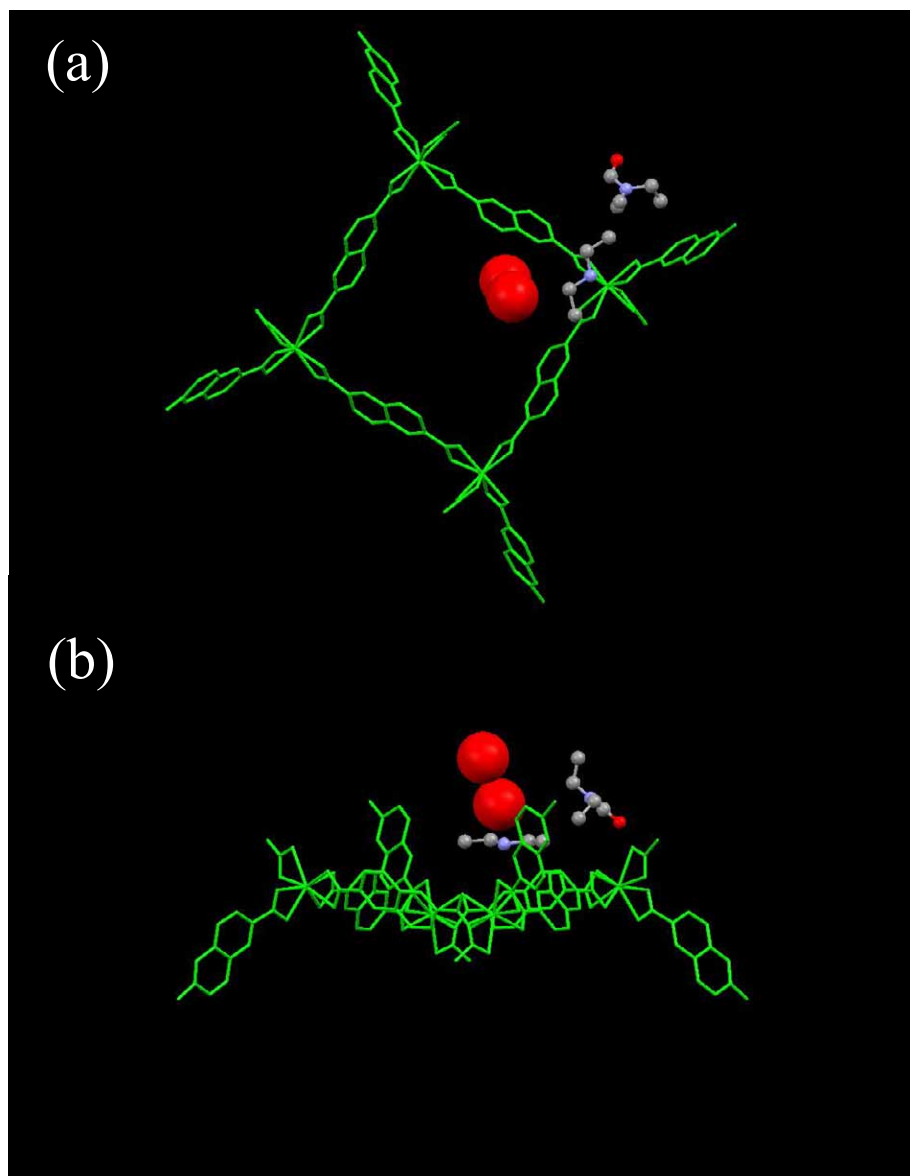


Figure S4. The 4-fold interpenetrated $4^3 \cdot 6^2 \cdot 8$ -gis network of **1**: a view along c -axis (a) and its tilted view (b). Solvates, Et_2NH_2^+ ions, and hydrogen atoms are omitted for clarity.

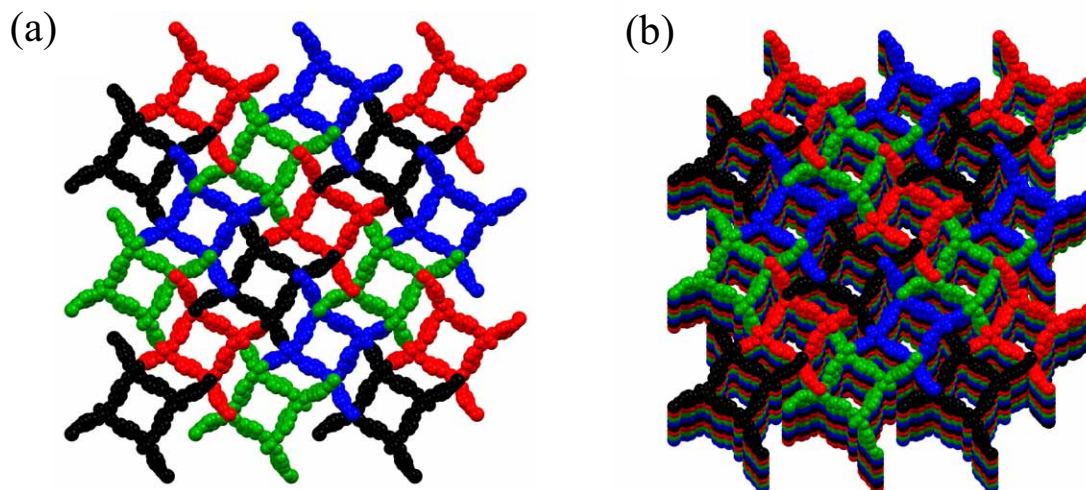


Figure S5. Pore size distribution curves obtained by the MP method. Both samples were activated at 120°C under high vacuum for 2 h.

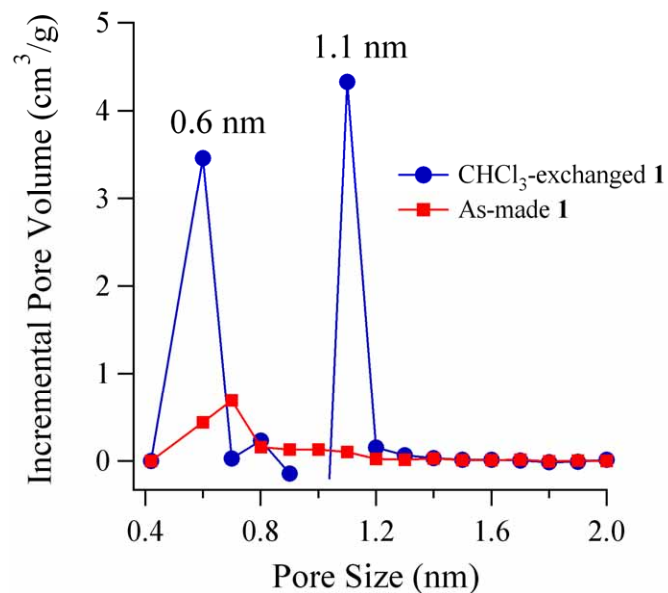


Figure S6. The PXRD patterns of **1** activated at various conditions with the relevant simulated patterns.

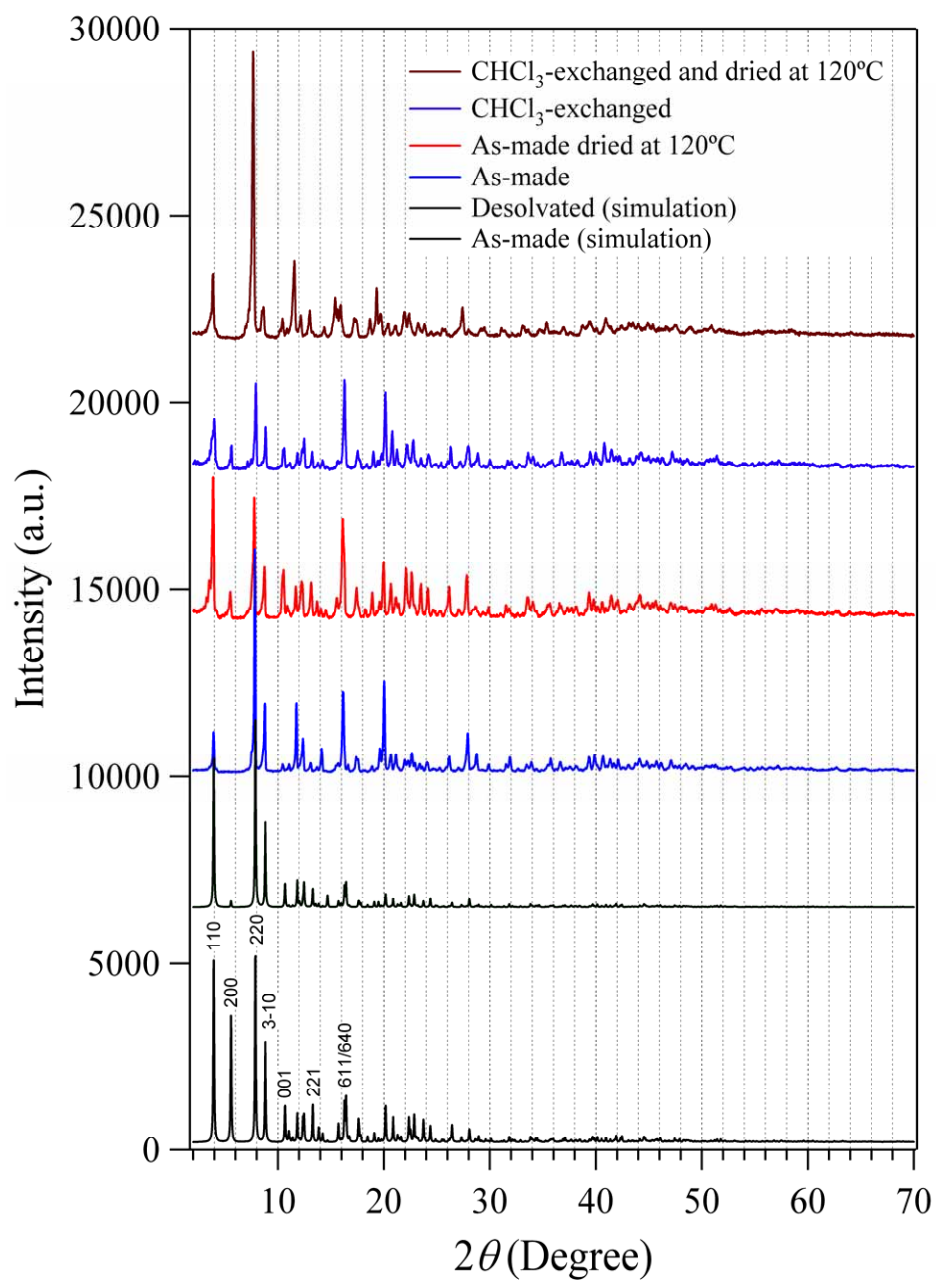


Figure S7. The optimized geometry with H₂ on site C calculated with the LDA.

